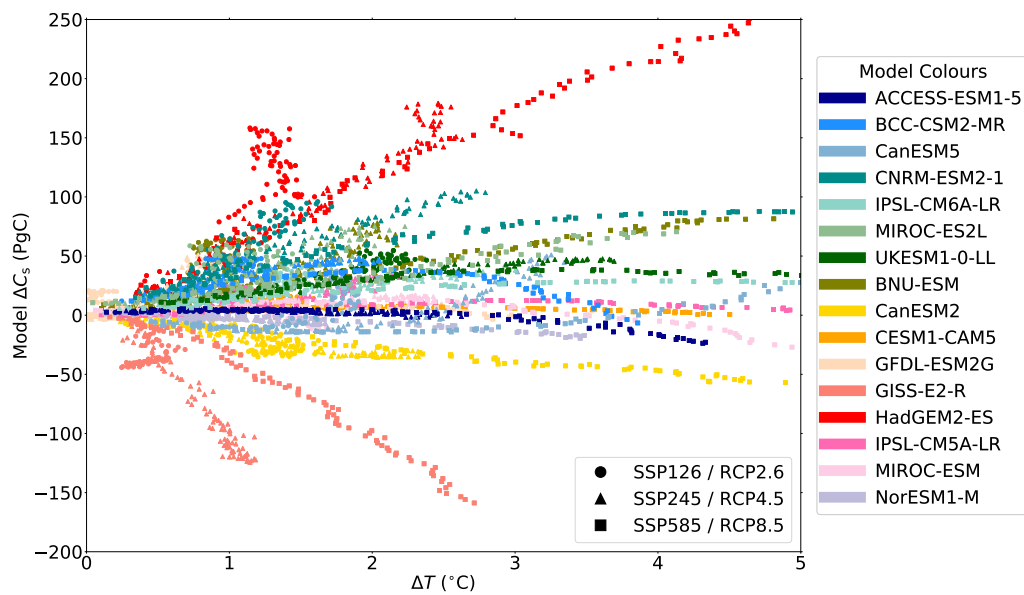
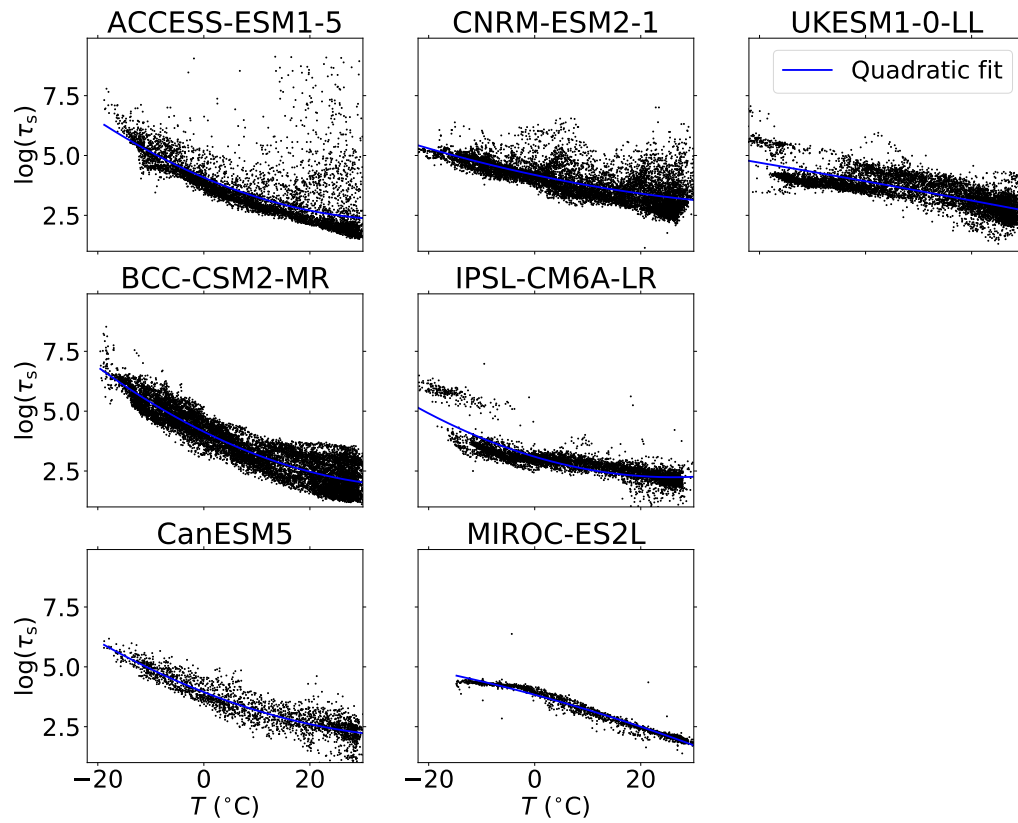


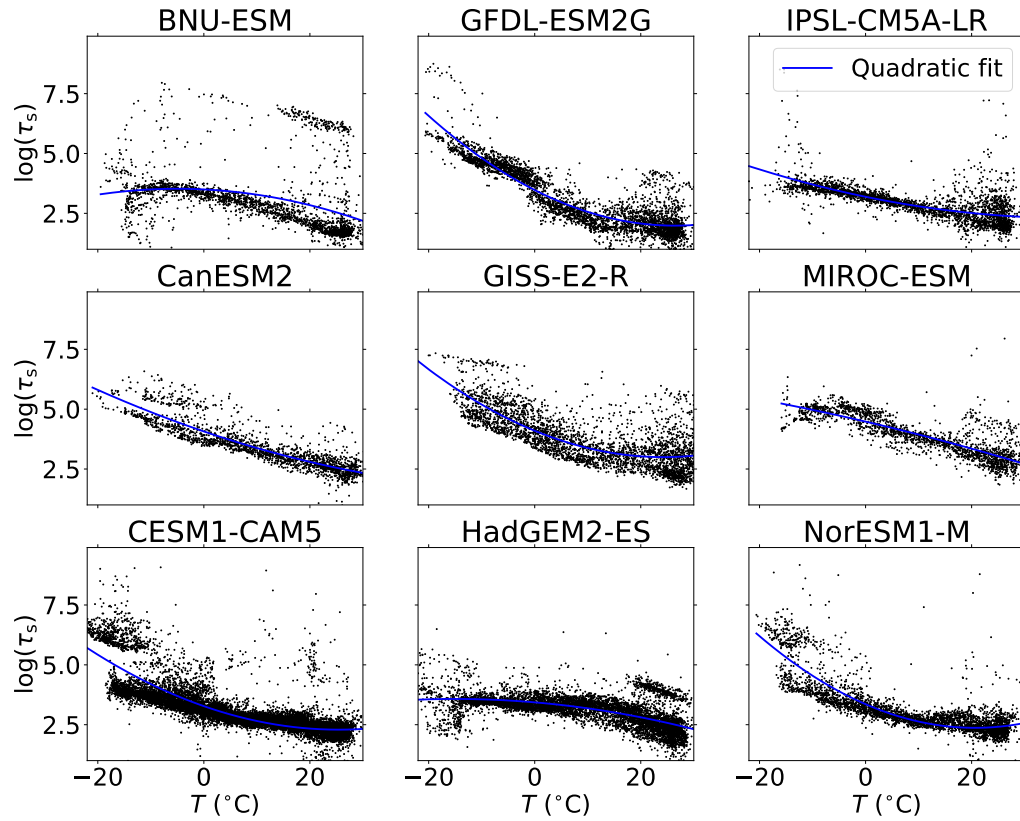
Supplementary Information for ‘A spatial emergent constraint on the sensitivity of soil carbon turnover to global warming’ by Varney et al.



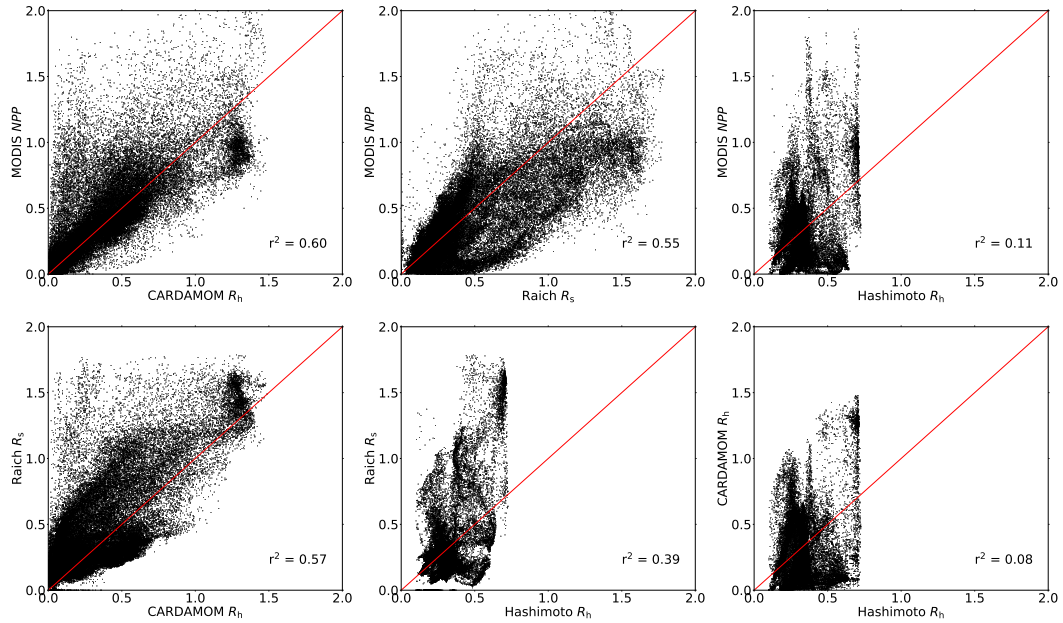
Supplementary Figure 1: **Uncertainties in future total soil carbon change.** The change in soil carbon, ΔC_s , against change in global mean temperatures, ΔT , diagnosed from sixteen Earth System Models (seven CMIP6 ESMs and nine CMIP5 ESMs), for three different future scenarios: SSP126, SSP245, SSP585, or RCP2.6, RCP4.5, RCP8.5 respectively.



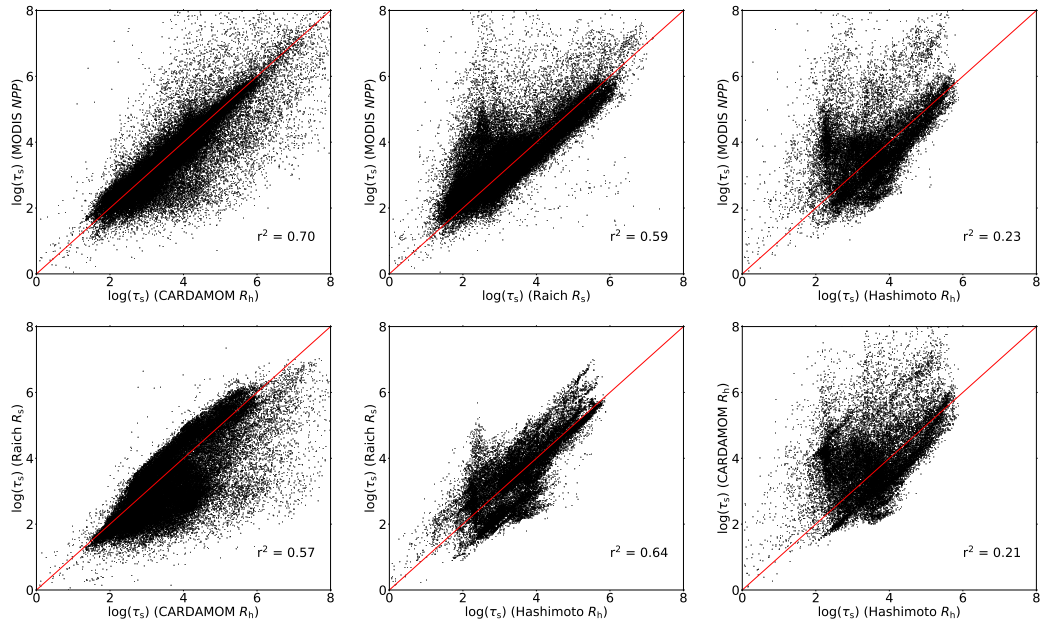
Supplementary Figure 2: **Deriving the CMIP6 model-specific $\log \tau_s$ -temperature relationships.** Scatter plots of the relationship between soil carbon turnover, $\log \tau_s$, and near surface air temperature, T , for each CMIP6 ESM considered in our study. The black points represent the individual grid points of data, and the blue lines show the spatial $\log \tau_s$ -temperature quadratic fits.



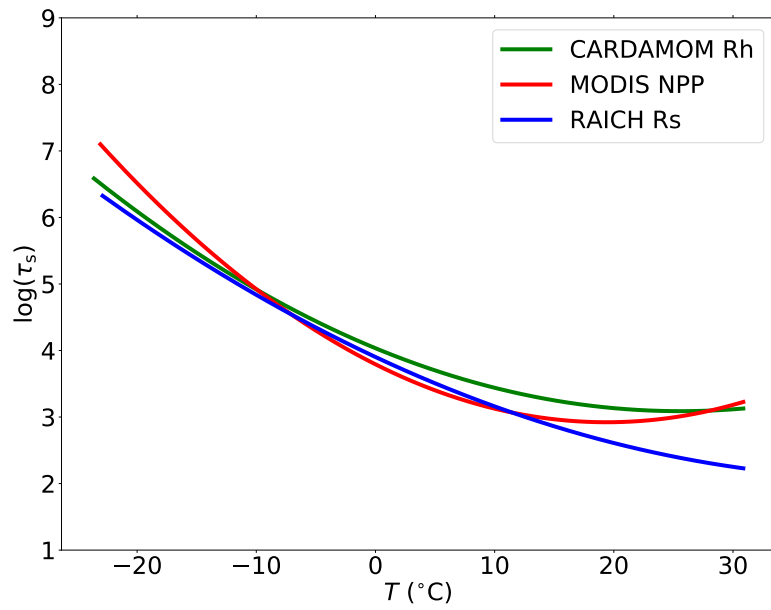
Supplementary Figure 3: **Deriving the CMIP5 model-specific $\log \tau_s$ -temperature relationships.** Scatter plots of the relationship between soil carbon turnover, $\log \tau_s$, and near surface air temperature, T , for each CMIP5 ESM considered in our study. The black points represent the individual grid points of data, and the blue lines show the spatial $\log \tau_s$ -temperature quadratic fits.



Supplementary Figure 4: **One to one comparisons of observational datasets.** Scatter plots showing one-to-one comparisons of all the observational datasets considered in this study against one another, including: CARDAMOM heterotrophic respiration (R_h) [1], MODIS net primary production (NPP) [2], Raich 2002 soil respiration (R_s) [3], and Hashimoto 2015 R_h [4]. The black data points represent the spatial data for each grid point, and the red lines show a one-to-one comparison. The respective r^2 correlation coefficients are stated on each figure panel.



Supplementary Figure 5: **One to one comparisons of $\log \tau_s$ for each observational dataset.** Scatter plots showing one-to-one comparisons of $\log \tau_s$ calculated using each of the observational datasets considered in this study: CARDAMOM heterotrophic respiration (Rh) [1], MODIS net primary production (NPP) [2], Raich 2002 soil respiration (Rs) [3], and Hashimoto 2015 Rh [4]. The black data points represent the spatial data for each grid point, and the red lines show a one-to-one comparison. The respective r^2 correlation coefficients are stated on each figure panel.



Supplementary Figure 6: **Comparison of the quadratic fits for different observational datasets.**

The spatial $\log \tau_s$ -temperature derived quadratic fits using our observational datasets: CARDAMOM Rh [1], MODIS NPP [2], and Raich 2002 soil respiration (Rs) [3].

Supplementary References

1. Bloom, A., Williams, M. *et al.* Cardamom 2001-2010 global carbon model-data fusion (mdf) analysis (2015).
2. Zhao, M., Heinsch, F. A., Nemani, R. R. & Running, S. W. Improvements of the modis terrestrial gross and net primary production global data set. *Remote sensing of Environment* **95**, 164–176 (2005).
3. Raich, J. W., Potter, C. S. & Bhagawati, D. Interannual variability in global soil respiration, 1980–94. *Global Change Biology* **8**, 800–812 (2002).
4. Hashimoto, S. *et al.* Global spatiotemporal distribution of soil respiration modeled using a global database. *Biogeosciences* **12**, 4121–4132 (2015).